Spin-Polarized Scanning Tunneling Microscopy: Breakthroughs and Highlights

Matthias Bode*

Abstract: The principle of scanning tunneling microscopy, an imaging method with atomic resolution capability invented by Binnig and Rohrer in 1982, can be adapted for surface magnetism studies by using magnetic probe tips. The contrast mechanism of this so-called spin-polarized scanning tunneling microscopy, or SP-STM, relies on the tunneling magneto-resistance effect, *i.e.* the tip–sample distance as well as the differential conductance depend on the relative magnetic orientation of tip and sample. To illustrate the working principle and the unique capabilities of SP-STM, this compilation presents some key experiments which have been performed on various magnetic surfaces, such as the topological antiferromagnet Cr(001), a double-layer of Fe which exhibits a stripe-domain pattern with about 50 nm periodicity, and the Mn monolayer on W(110), where the combination of experiment and theory reveal an antiferromagnetic spin cycloid. Recent experimental results also demonstrate the suitability of SP-STM for studies of dynamic properties, such as the spin relaxation time of single magnetic nanostructures.

Keywords: Spin-polarized scanning tunneling microscopy (SP-STM)

1. Introduction

With its ability to image surfaces in real space with atomic resolution, scanning tunneling microscopy (STM) has had an enormous impact on surface science. It not only became possible to study and critically evaluate the effectiveness of various surface preparation techniques, which led to an tremendous improvement of surface quality, the huge impact of STM also played a decisive role in the advent of nanosciences, *i.e.* the attempt to understand, control, and utilize the often extraordinary physical properties of small objects.

The properties of small magnetic particles and thin films played a decisive role in the race for high-density data storage devices. Their analysis and optimization requires high-resolution magnetically sensitive imaging techniques. Also from a

basic science point of view magnetic imaging techniques were of key importance for understanding the formation of magnetic domain structures and the interaction of magnetic domains with structural features. Unfortunately, with the exchange length of the ferromagnetic 3d-metals Fe, Co, and Ni being in the 10-nm range, conventional magnetic imaging techniques, such as the Bitter technique, the magneto-optical Kerr effect,[1] Lorenz microscopy,[2] or magnetic force microscopy,[3] do not offer sufficient resolution to allow for a detailed analysis of *e.g.* domain wall profiles. In particular, the atomic scale magnetization pattern of antiferromagnetic surfaces was and still is inaccessible to these methods.

In this context magnetically sensitive STM, or so-called spin-polarized STM (SP-STM), opened new prospects, as – compared with the above-mentioned techniques – it gained roughly one order of magnitude in resolution. Thereby, it became possible to image spin structures in real space on the atomic scale which not only allowed new insight into magnetic properties on the nano-scale but also led to the discovery of previously unknown complex spin structures in thin films.

2. Methods and Materials

It was Binnig and Rohrer's achievement to realize that the exponential decay of the electron wave function in the vacuum tunneling barrier between two

electrically conducting electrodes can be utilized for a new type of ultra-high resolution microscopy.[4–6] Very soon after their groundbreaking experiments new ideas for advanced measurement modes were presented. These not only included various electron spectroscopy modes[7–9] but also a proposal of Pierce[9] to locally probe the magnetic orientation of the sample by making the tunneling process sensitive to the electron spin.

In fact, spin-polarized electron tunneling in planar junctions was already known since Tedrow and Meserey had performed experiments with superconducting-ferromagnetic planar junctions.[10–12] Since the tunneling current can be described by the overlap of the local density of states (LDOS) close to the Fermi level and since – in the absence of inelastic processes – the electron spin has to be conserved during the tunneling process, the current flow through a tunneling barrier depends on the relative magnetic orientation of the two electrodes. Consequently, the preparation of suitable tips with a high degree of spin polarization was crucial for the successful development of spin-polarized scanning tunneling microscopy (SP-STM).

Early attempts by Johnson and Clarke[13] to prove the concept of spin-polarized STM under ambient conditions were focused on controlling the magnetization direction of the two electrodes by their shape anisotropy. The sample was a toroid-shaped permalloy ($Ni_{79}Fe_{21}$) single crystal and the tip consisted of a Ni crys-

*Correspondence: Prof. Dr. M. Bode
Fakultät für Physik und Astronomie
Lehrstuhl für Experimentelle Physik II
Am Hubland
D-97074 Würzburg, Germany
Tel.: +49 931 318 3218
E-mail: bode@physik.uni-wuerzburg.de

tal positioned within the gap of a magnetic yoke. Indeed, a modulation of the tunneling current was observed when alternating the sample magnetization. However, competing effects such as magnetic forces and magnetostriction could not be excluded.

Since SP-STM, like any other STM mode of operation, is extremely surface sensitive, it was obvious that any successful experiment would require ultrahigh vacuum (UHV) conditions to allow the preparation of clean surfaces. In addition, suitable magnetic tip materials which offer a high degree of spin-polarization had to be identified. In hindsight, three concepts proved to be successful: ferromagnetic thin film tips,[14] low-coercivity and low-magnetostriction bulk tips,[15,16] and antiferromagnetic tips.[17]

3. Results and Discussion

The main challenge during the development of SP-STM was to identify a suitable test sample which exhibits a well-defined surface magnetic domain structure. Here the (001) surface of chromium (Cr) played a key role. Local density approximation calculations performed by Blügel *et al*.[18] predicted a ferromagnetic coupling within the (001) surface plane. However, the results also showed that the inter-plane coupling, *i.e.* perpendicular to the surface, is antiferromagnetic. Blügel *et al*. realized that the presence of atomic steps on the surface would expose different (001) planes to the surface, resulting in a surface magnetization that alternates at every surface atomic step edge. This magnetic structure was coined 'topological antiferromagnetism'.

Wiesendanger *et al*.[19] recognized that this intimate link between the topographic and magnetic structure of Cr(001) would allow spin-averaged from spin-dependent contributions to be reliably differentiated. Their results are shown in Fig. 1(a). While the topographic step height of 0.14 nm was measured with a non-magnetic W tip (upper left panel), alternating apparent step heights of 0.12 nm and 0.16 nm were observed with a magnetic CrO_2 tip.[19]

This observation can be explained by the response of the feedback circuit on the spin-polarized contribution to the tunneling current as schematically represented in the upper panel of Fig. 1(b). If tip and sample are magnetized in opposite directions their respective minority and majority spin channels do not match. This would, at a given tip–sample distance, result in a reduction of the tunneling current I_t. However, the feedback circuit ensures that I_t remains constant which is achieved by reducing the tip–sample distance d_A correspondingly. The opposite is true for the
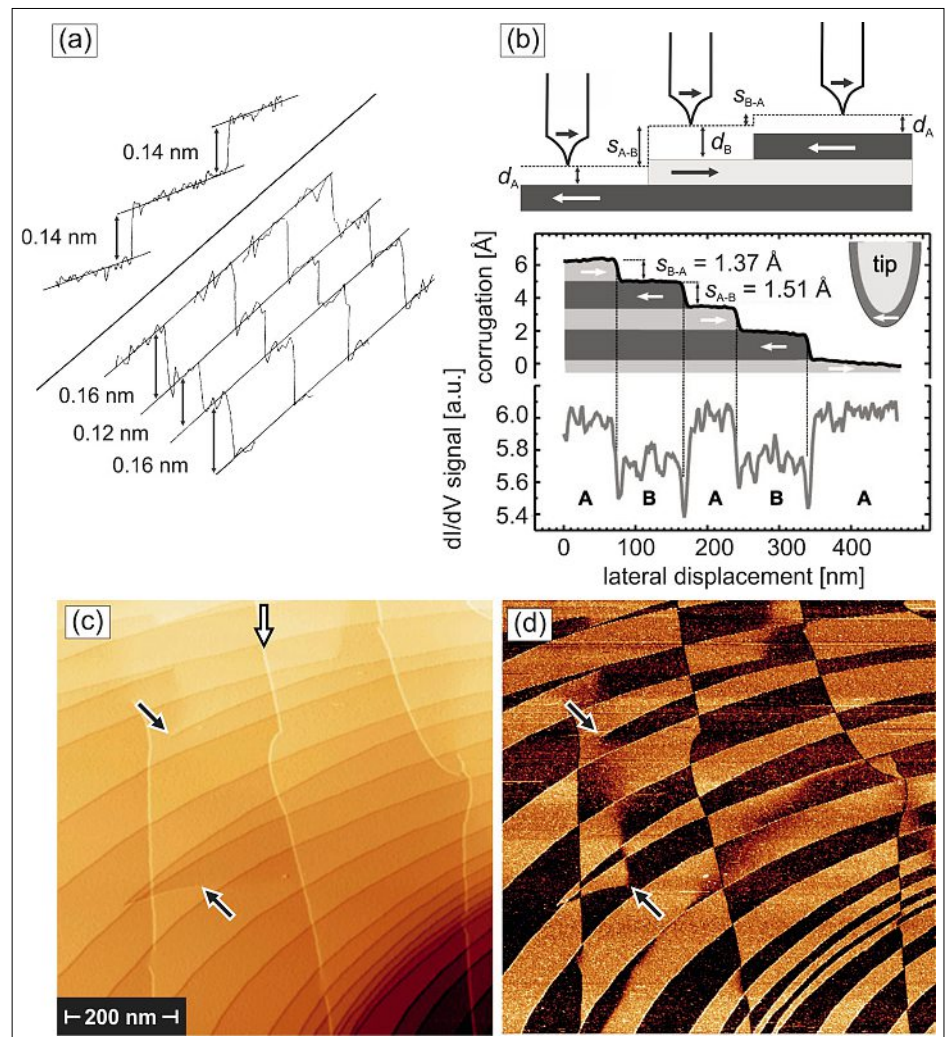

Fig. 1. (a) Line scans taken on Cr(001). While the topographic step height is observed with a non-magnetic W tip (top left), a subtle modulation of the apparent step height shows up if a magnetic tip, bulk CrO_2 in this case, is used (bottom left). (b) This modulation is explained by a spin-dependent contribution to the tunneling current between a magnetic tip and the layered antiferromagnetic sample (top panel). Later experiments performed with thin film tips showed that the modulation of the apparent step height is accompanied by a modulation of the differential conductivity, dI/dV (bottom panel). The simultaneous measurement of (c) topography images and (d) dI/dU maps allows the clear separation of topographic and magnetic information. Data in (a) and (b) courtesy of R. Wiesendanger, ref. [19] and M. Kleiber, ref. [20], copyright 1990 and 2000 by The American Physical Society.

adjacent terrace where the sample exhibits a magnetization direction parallel to the tip. Here minority and majority channels match and I_t would increase, which is again compensated by the feedback, this time by increasing the tip–sample distance d_B. As can be seen in the upper panel of Fig. 1(b) the variation of the tip–sample distance results in a characteristic variation of the apparent step heights; while the step edge s_{A-B} appears lower than the topographic step height, step edge s_{B-A} appears higher.

The problem of this mode of operation is that both the topographic and the magnetic contributions are still part of the same data, *i.e.* the tip height. As we will see below this mode of operation is adequate for imaging antiferromagnets on the atomic scale, but it is not suitable for mapping magnetic domains. Kleiber *et al*.

showed[20] that spin-polarized scanning tunneling spectroscopy allows for a better separation of topography and magnetic domain structure.

In this mode, the surface domain structure can be mapped simultaneously with the topography by recording the differential conductance (dI/dU) between tip and sample. The line section in the lower panel of Fig. 2(b) shows two line sections of the topography and the dI/dU signal taken while the tip was scanned across four single-atomic step edges of a Cr(001) surface. While the spin-dependent contribution to the tunneling current causes a minor variation in the apparent step height only (s_{A-B} versus s_{B-A}), a clear modulation between two discrete levels of the dI/dU signal can be recognized by comparing Cr terraces of type A and B.

Indeed, differential conductance mapping with magnetically coated tips enables high-resolution studies of the surface domain structure of single-crystalline surfaces. Figs. 1(c) and (d) show the topography and the simultaneously measured differential conductance, respectively, as measured with an Fe-coated probe tip on a Cr(001) surface. The scanned area amounts to 800 nm × 800 nm. While the overall miscut leads to mono-atomic step edges oriented from the bottom left to the upper right of the scan area, screw and edge dislocations lead to a more complex surface topography.

As mentioned above, the topology and surface magnetic structure are closely linked in Cr(001). Consequently, these features substantially influence the surface domain structure. In particular, the formation of domain walls can be observed between pairs of screw dislocations; one such example is marked by two black arrows. Edge dislocations (one example marked by a white arrow) effectively lead to additional step edges which are misaligned with respect to the miscut-induced steps. Quantitative analysis revealed that the domain wall width of Cr(001) amounts to about 150 nm,[20] a result previously inaccessible with conventional magnetic imaging techniques (not shown here).

One issue of scanning probe methods that involve ferromagnetic tips is the stray-field mediated interaction between the tip and the sample which might influence the sample's domain structure. For magnetic force microscopy this perturbation has clearly been identified, especially at small tip–sample separations.[21] In the SP-STM measurements presented above this issue was avoided by scanning an antiferromagnetic sample which is intrinsically inert against stray fields up to the spin-flop transition which occurs much higher field strength only. For ferromagnetic samples, however, the tip-induced Zeemann energy may alter the sample's domain structure, especially if it is magnetically soft.

An example of the impact of an tip's stray field on the magnetic domain structure during an SP-STM measurement is presented in Fig. 2. This measurement was performed with the intent to understand field-dependent changes in the stripe domain pattern of Fe double-layer films on W(100). Sample preparation is performed by e-beam evaporation of an equivalent of two atomic layers (AL) onto the W(110) substrate held at slightly elevated temperature (≈400 K). Almost perfect step edge decoration leads to a sample topography which is still dominated by the stepped substrate. The images were obtained with a tip coated by a GdFe film with a total thickness of about 16 AL. It was prepared by co-deposition of Gd (14 AL) and Fe (2 AL).
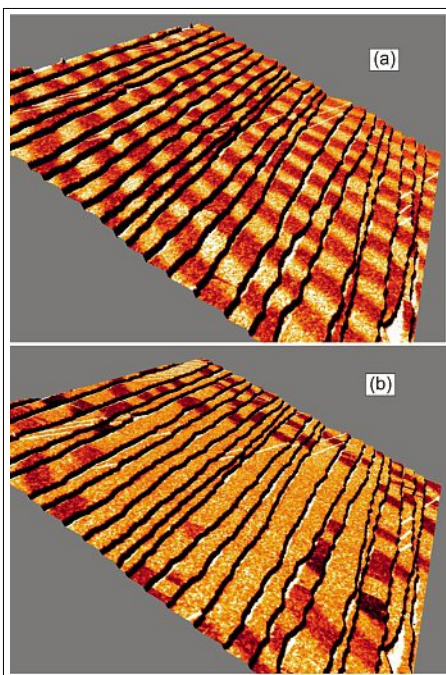

Fig. 2. Stripe domain pattern of the Fe double-layer on a stepped W(110) substrate (scan area: 500 nm × 500 nm) as scanned with a ferromagnetic GdFe tip before (a) and after a field sweep. During the field sweep the central 200 nm × 200 nm area was repeatedly scanned. The superposition of the macroscopic external and the local tip field leads to the annihilation of the dark domains which were oriented opposite to the field direction.

To improve film stability, upon deposition the coating was gently annealed at about 600 K for 4 min.

Fig. 2(a) presents data measured prior to the application of any magnetic field. The image is a superposition of topographic (shown as rendered perspective data) and magnetic information (color-coded differential conductivity dI/dU). The displayed surface area is 500 nm × 500 nm. The step edge and terrace structure of the sample topography can be clearly recognized. As can be clearly seen in Fig. 2(a) the sample surface initially exhibits a well-defined stripe-domain pattern that consists of perpendicular domains with alternating up (bright) and down (dark) magnetization. This domain structure is stabilized by the Dzyaloshinskii-Moriya interaction[22] and has been the subject of numerous investigations.[23–28]

During the following course of the measurements the central region of Fig. 2(a), 200 nm × 200 nm in size, was repeatedly scanned under the influence of perpendicular magnetic fields with a strength of up to 700 mT. Then the external field was released and the same surface area was imaged again. The resulting data are shown in Fig. 2(b). By comparing Figs. 2(a) and (b) it becomes obvious that the external field has modified the surface domain structure.

However, significant differences between the central region and the surrounding areas can be recognized. While the density of domains of the outer (not scanned) areas is somewhat reduced, the total annihilation of dark domains is observed in the central part of the image, *i.e.* where the tip scanned across the sample surface while a field was applied.

Detailed analysis showed that this modification of the surface domain structure is caused by the superposition of the tip's local stray field with the externally applied magnetic field.[17] Estimates show that a magnetically coated tip at short distances of about 1 nm, which corresponds to the approximate tip–sample distance within an STM, produces a local field of several 10 mT in strength with strong gradients and in-plane components.[17] If the external field is close to the saturation field of the sample, this relatively small field very efficiently modifies the surface domain structure.[17]

As has been shown in refs. [17] and [29] this undesirable effect can be avoided by using antiferromagnetic thin film or bulk tips, respectively. In general, antiferromagnets are compensated and possess no net magnetization. However, due to the potential existence of uncompensated moments at or close to the apex this might not be entirely true for tapered objects, such as an STM tip. Although the stray-field-induced tip–sample interaction is greatly reduced for antiferromagnetic tips,[17] some experiments show that they interact with strong external fields (several Tesla),[30] indicating the existence of uncompensated moments.

As mentioned above it is the STM's ability to resolve surfaces in real space and with atomic resolution which makes it unique among other surface science analysis tools and particularly suitable for many aspects of nanoscience. Accordingly, spin-polarized STM is able to resolve atomic scale spin structures. In solid-state physics antiferromagnets resemble the smallest possible magnetic periodicity, as their magnetization direction alternates between adjacent atoms.

Indeed, it has been shown in numerous experiments that SP-STM enables atomic spin resolution studies of antiferromagnetic surfaces.[31–34] In these experiments details of antiferromagnetic domain and domain wall structures in collinear[31–33] and frustrated spin arrangements, such as the Néel structure,[34] were revealed.

The ability to image spin structures on the atomic scale also allowed for the discovery of very complex compensated magnetic ordering phenomena in systems with broken inversion symmetry. Although predicted theoretically for a long time,[35] these spin structures in ultra-thin films

and nanostructures were invisible for conventional far-field magnetic measurement methods. While spatially averaging techniques like neutron diffraction are in general capable of detecting periodic spin structures, such as spin spirals or helical order, in the volume of magnetic materials, the small cross section of neutrons with solids prohibits the application of this technique to single magnetic layers with a thickness of a few atomic layers only or even single nanostructures.

One example of a complex spin structure discovered with SP-STM is shown in Fig. 3(a). The sample consists of a Mn monolayer on a W(110) substrate. It is well-known from earlier investigations that the growth of Mn on W(110) is pseudomorphic, *i.e.* Mn atoms occupy W lattice sites and thereby mimic the substrate's structure.[36] The measurements have been performed with an Fe-coated tungsten tip which, in the absence of an external magnetic field, is sensitive to the sample's in-plane magnetization. Besides a few adsorbates, which appear as bright and dark spots, the constant-current image of Fig. 3(a) (scan area 20 nm × 20 nm) is dominated by narrow stripes running along the [001]-direction.

These stripes are caused by the tunneling magneto-resistance effect between the magnetic tip and the sample. When tip and sample atom underneath the tip apex are parallel the respective majority channels are populated with spins of the same quantization axis. The resulting enhanced tunnel conductance is compensated by the feedback loop, which retracts the tip from the sample surface to keep the total tunneling current constant. Correspondingly, the tip is approached towards the surface in the case of an antiparallel orientation.

In the line section which was drawn along the black line in Fig. 3(a), plotted in Fig. 3(b), it can be recognized that this spin-dependent contribution to the tunneling current results in a 'magnetic corrugation' of up to 15 pm. The periodicity between two maxima (minima), which correspond to the bright (dark) stripes in Fig. 3(a), amounts to 4.45 ± 0.04 Å. This value is consistent with the W [001] lattice constant of 4.48 Å and can be explained by an antiferromagnetic spin arrangement between adjacent [001] rows. If the measurements were performed with a nonmagnetic tip the Mn atoms, regardless of their magnetization direction, would be indistinguishable and would all appear with an identical apparent height.

However, in addition to a short wavelength oscillation the line section of Fig. 3(b) also reveals a modulation of the magnetic corrugation which takes place on a length scale of about 6 nm. This observation is inconsistent with a simple collinear
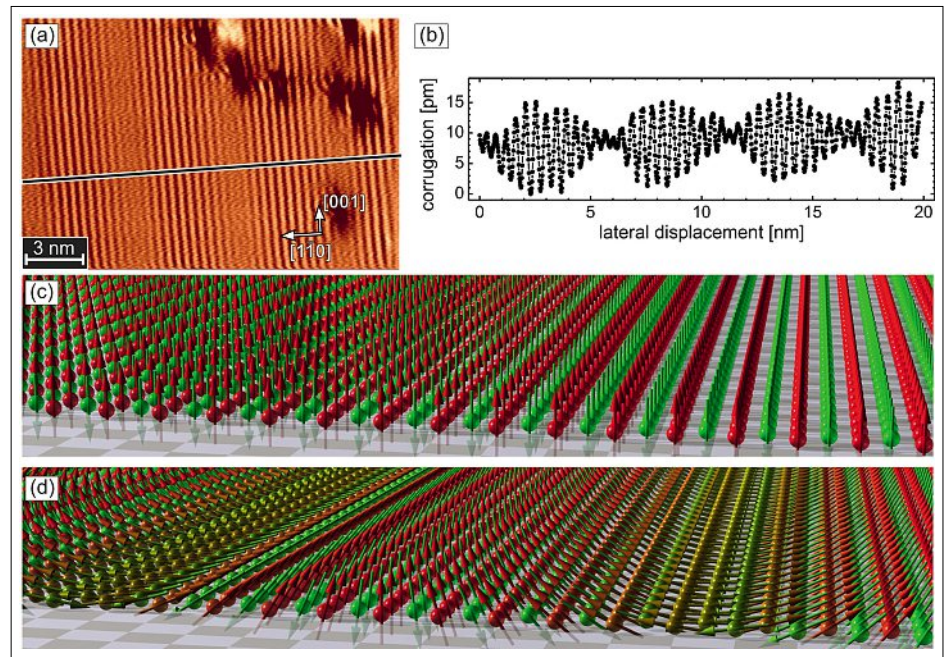

Fig. 3. (a) Constant-current SP-STM image of a Mn monolayer on W(110) as measured with an Fe-coated probe tip at *T* =13 K. (b) The line section drawn along the surface [001] direction reveal two oscillations. While the 'rapid' oscillation exhibits a periodicity of 4.45 ± 0.04 Å and is caused by the almost antiferromagnetic coupling between adjacent [001] rows, it is superimposed by a 'slower' intensity modulation (periodicity about 6 nm). The latter is inconsistent with a simple row-wise antiferromagnetic order as shown in (c). Instead, theoretical calculations show that the magnetization axis of the Mn monolayer periodically changes between in-plane and out-of-plane (d) due to the Dzyaloshinskii-Moriya interaction.[34]

antiferromagnetic spin structure as schematically shown in Fig. 3(c) (note that the out-of-plane magnetization direction was selected for illustrational purposes only; an Fe-coated tip would only be sensitive to the in-plane magnetization direction).

Instead, experiments in which the tip magnetization was intentionally influenced by an applied external field in combination with *ab initio* density functional theory calculations revealed that the spin structure is much more complex.[37] The coupling angle between adjacent [001] rows is not perfectly antiparallel but amounts to about 172°. Thereby, the local magnetization axis slowly oscillates like a cycloid between in-plane and the out-of-plane direction and gives rise to the modulated magnetic amplitude in Fig. 3(a).

Going beyond static properties, recent experiments aim for an understanding of dynamic properties of magnetic nanostructures. Examples include magnetic phase transitions,[38] magnon dispersion in magnetic nanostructures,[39] or even atomic scale spin excitations.[40] Pioneering all-electrical pump-probe experiments were performed by Loth *et al.*[40,41] on the electron spin relaxation times in single atomic scale nanostructures. In these experiments, the scheme of which is illustrated in Fig. 4(a), the initial state spin quantization axis of the magnetic tip and the sample spin

is set by an external magnetic field of 7 T. This equilibrium state is excited by a pump pulse with a voltage amplitude which exceeds the sample's spin excitation energy.

The excitation (pump) pulse is followed by a probe pulse with a variable delay. To avoid further excitations of the sample system it is important that the amplitude of the probe pulse is significantly lower than the spin excitation threshold. Similar to the above-mentioned static spin-polarized STM experiments, due to the magneto-resistance effect the tunneling current which flows between the tip and the sample during the probe pulse will depend on their relative orientation of tip and sample.

By repeating this stroboscopic measurement scheme at various pump-probe delay times the spin relaxation time can be determined. A result of a typical measurement performed on a single nanostructure consisting of a Fe/Cu dimer is presented in Fig. 4(b). At large negative delay times the probe pulse precedes the pump pulse and therefore detects the undistorted system (variation of the tunneling current $\Delta I = 0$). This regime is followed by the blue shaded time interval where pump and probe pulse overlap. Only after this regime the relaxation of the sample spin can be clearly recognized as an exponential recovery of the SP-STM signal. Fitting the experimental data yields a spin relaxation time of 154 ns.
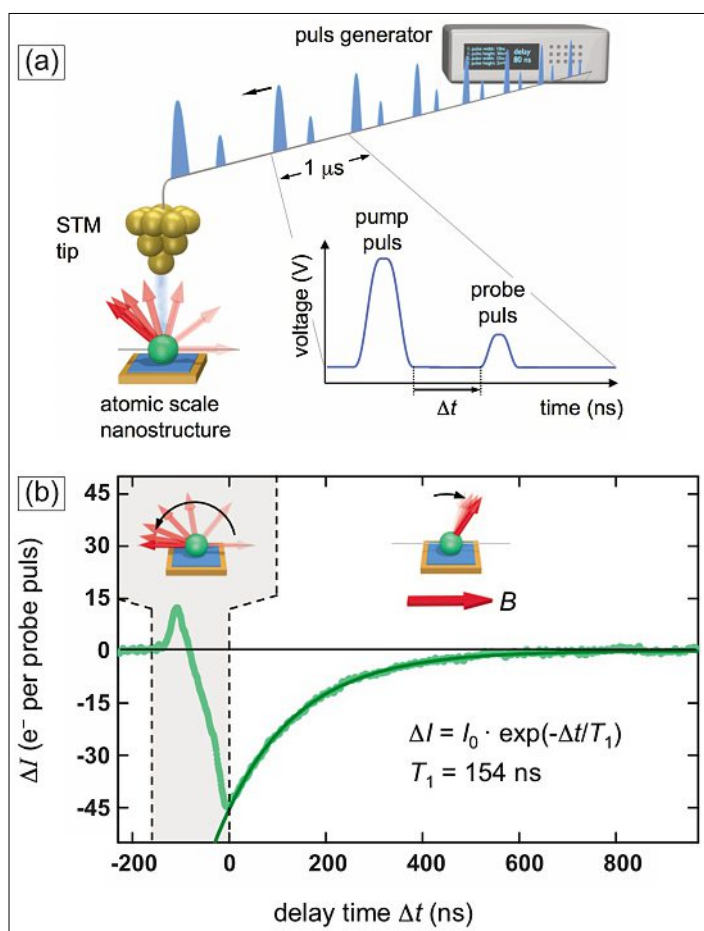
Fig. 4. (a) Illustration of the imaging the spin relaxation time through an all-electrical pump-probe experiment. (b) Plot of the variation of the tunneling current ΔI versus the pump-probe delay time as determined in a stroboscopic measurement on a single Fe/Cu-dimer (light green). The experimental data are fit by an exponential (dark green), resulting in a relaxation time $T_1 = 154$ ns. Courtesy of S. Loth, ref. [41], copyright 2011 by Wiley.

4. Summary

By making use of a relatively simple modification, *i.e.* the use of magnetic probe tips, the scanning tunneling microscope invented by Binnig and Rohrer in the 1980s can be made sensitive to the spin of the tunneling electron. Based on this measurement principle, SP-STM allows for the imaging magnetic domains in ferromagnets with unprecedented spatial resolution. Even more important, on antiferromagnetic surfaces and in magnetic nanostructures, atomic spin resolution allows the understanding of static and dynamic magnetic properties with previously unachievable precision.

[1] A. Hubert, R. Schäfer, 'Magnetic domains: the analysis of magnetic microstructures', Springer Berlin, Heidelberg, **2000**.
[2] A. K. Petford-Long, J. N. Chapman, 'Lorentz microscopy', in 'Magnetic Microscopy of Nanostructures', Eds. H. Hopster, H. P. Oepen, Springer Berlin, Heidelberg, **2005**.
[3] A. Schwarz, M. Bode, R. Wiesendanger, 'Scanning Probe Techniques: MFM and SP-STM', in 'Handbook of Magnetism', Vol. 3, Eds. H. Kronmüller, S.S.P. Parkin, Wiley, **2006**.
[4] G. Binnig G, H. Rohrer, *Helv. Phys. Acta* **1982**, *55*, 726.
[5] G. Binnig, H. Rohrer, C. Gerber, E. Weibel, *Appl. Phys. Lett.* **1982**, *40*, 178.
[6] G. Binnig, H. Rohrer, C. Gerber, E. Weibel, *Phys. Rev. Lett.* **1983**, *50*, 120.
[7] N. D. Lang, *Phys. Rev. B* **1986**, *34*, 5947.
[8] W. J. Kaiser, R. C. Jaklevic, *Surface Science* **1987**, *181*, 55.
[9] D. T. Pierce, *Phys. Scr.* **1988**, *38*, 291.
[10] R. Meservey, P. M. Tedrow, P. Fulde, *Phys. Rev. Lett.* **1970**, *25*, 1270.
[11] P. M. Tedrow, R. Meservey, *Phys. Rev. B* **1973**, *7*, 318.
[12] R. Meservey, P. M. Tedrow, *Phys. Rep.* **1994**, *238*, 173.
[13] M. Johnson, J. Clarke, *J. Appl. Phys.* **1990**, *67*, 6141.
[14] M. Bode, M. Getzlaff, R. Wiesendanger, *Phys. Rev. Lett.* **1998**, *81*, 4256.
[15] W. Wulfhekel, J. Kirschner, *Appl. Phys. Lett.* **1999**, *75*, 1944.
[16] U. Schlickum, W. Wulfhekel, J. Kirschner, *Appl. Phys. Lett.* **2003**, *83*, 2016.
[17] A. Kubetzka, M. Bode, O. Pietzsch, R. Wiesendanger, *Phys. Rev. Lett.* **2002**, *88*, 057201.
[18] S. Blügel, D. Pescia, P. H. Dederichs, *Phys. Rev. B* **1989**, *39*, 1392.
[19] R. Wiesendanger, H.-J. Güntherodt, G. Güntherodt, R. J. Gambino, R. Ruf, *Phys. Rev. Lett.* **1990**, *65*, 247.
[20] M. Kleiber, M. Bode, R. Ravlic, R. Wiesendanger, *Phys. Rev. Lett.* **2000**, *85*, 4606.
[21] U. Hartmann, *Ann. Rev. Mater. Sci.* **1999**, *29*, 53.
[22] M. Heide, G. Bihlmayer, S. Blügel, *Phys. Rev. B* **2008**, *78*, 140403.
[23] O. Pietzsch, A. Kubetzka, M. Bode, R. Wiesendanger, *Phys. Rev. Lett.* **2000**, *84*, 5212.
[24] M. Bode, O. Pietzsch, A. Kubetzka, S. Heinze, R. Wiesendanger, *Phys. Rev. Lett.* **2001**, *86*, 2142.
[25] M. Bode, S. Heinze, A. Kubetzka, O. Pietzsch, X. Nie, G. Bihlmayer, S. Blügel, R. Wiesendanger, *Phys. Rev. Lett.* **2002**, *89*, 237205.
[26] A. Kubetzka, O. Pietzsch, M. Bode, R. Wiesendanger, *Phys. Rev. B* **2003**, *67*, 020401.
[27] K. von Bergmann, M. Bode, A. Kubetzka, M. Heide, S. Blügel, R. Wiesendanger, *Phys. Rev. Lett.* **2004**, *92*, 046801.
[28] E. Y. Vedmedenko, A. Kubetzka, K. von Bergmann, O. Pietzsch, M. Bode, J. Kirschner, H. P. Oepen, R. Wiesendanger, *Phys. Rev. Lett.* **2004**, *92*, 077207.
[29] A. Schlenhoff, S. Krause, G. Herzog, R. Wiesendanger, *Appl. Phys. Lett.* **2010**, *97*, 083104.
[30] G. Rodary, S. Wedekind, H. Oka, D. Sander, J. Kirschner, *Appl. Phys. Lett.* **2009**, *95*, 152513.
[31] S. Heinze, M. Bode, A. Kubetzka, O. Pietzsch, X. Nie, S. Blügel, R. Wiesendanger, *Science* **2000**, *288*, 1805.
[32] H. Yang, A. R. Smith, M. Prikhodko, W. R. L. Lambrecht, *Phys. Rev. Lett.* **2002**, *89*, 226101.
[33] M. Bode, E. Y. Vedmedenko, K. von Bergmann, A. Kubetzka, P. Ferriani, S. Heinze, R. Wiesendanger, *Nature Materials* **2006**, *5*, 477.
[34] C. L. Gao, W. Wulfhekel, J. Kirschner, *Phys. Rev. Lett.* **2008**, *101*, 267205.
[35] A. Bogdanov, A. Hubert, *J. Magn. Magn. Mater.* **1994**, *138*, 255.
[36] M. Bode, S. Heinze, A. Kubetzka, O. Pietzsch, M. Hennefarth, M. Getzlaff, R. Wiesendanger, X. Nie, G. Bihlmayer, S. Blügel, *Phys. Rev. B* **2002**, *66*, 014425.
[37] M. Bode, M. Heide, K. von Bergmann, P. Ferriani, S. Heinze, G. Bihlmayer, A. Kubetzka, O. Pietzsch, S. Blügel, R. Wiesendanger, *Nature* **2007**, *447*, 190.
[38] P. Sessi, N. P. Guisinger, J. R. Guest, M. Bode, *Phys. Rev. Lett.* **2009**, *103*, 167201.
[39] C. L. Gao, A. Ernst, G. Fischer, W. Hergert, P. Bruno, W. Wulfhekel, J. Kirschner, *Phys. Rev. Lett.* **2008**, *101*, 167201.
[40] S. Loth, M. Etzkorn, C. P. Lutz, D. M. Eigler, A. J. Heinrich, *Science* **2010**, *329*, 1628.
[41] S. Loth, M. Morgenstern, W. Wulfhekel, *Phys. unserer Zeit* **2011**, *42*, 168.